



Synergistic antimicrobial activity of N-methyl substituted pyrrolidinium-based ionic liquids and melittin against *Gram-positive* and *Gram-negative* bacteria

Juhi Saraswat¹ · Badr Aldahmash² · Suliman Yousef AlOmar³ · Khalid Imtiyaz⁴ · M. Moshahid Alam Rizvi⁴ · Rajan Patel¹

Received: 7 July 2020 / Revised: 13 October 2020 / Accepted: 28 October 2020
© Springer-Verlag GmbH Germany, part of Springer Nature 2020

Abstract

In pharmaceutical industry, the prodrug approaches and drug-drug conjugates are being now vastly used to optimize the efficacy of the drugs for multipurpose. The combination or conjugation of antimicrobials agents with natural antimicrobials may lead to better synergistic antimicrobial activity. Currently, many publications show the potential of ionic liquids (ILs) as novel antimicrobials and even as active pharmaceutical ingredients. The current study showed the synthesis of novel pyrrolidinium-based ILs (C_x , $x = 4, 6, 8, 10, 12$) and their antibacterial activity alone and in combination with antimicrobial peptide, melittin (MEL), against clinically relevant microorganism, *E. coli* and *S. aureus*. The cytotoxicity of synthesized ILs was administered on HEK 293 cell line using MTT assay. The obtained results showed the dependency of antibacterial activity of ILs on alkyl chain length ($C_4 < C_6 < C_8 < C_{10} < C_{12}$). The remarkable improvement in the antibacterial efficiency of MEL was seen with ILs; however, antibacterial effect is more pronounced with IL having large alkyl chain length (C_8 , C_{10} , and C_{12}) at their minimal concentration with MEL to disrupt the cell membrane. In addition, the binding study and haemocompatibility results showed favourable biocompatibility and stability which could potentially improve its utility for the biomedical field.

Key points

- The combination of melittin and pyrrolidinium-based ILs showed improved antibacterial activity against *E. coli* and *S. aureus* which may be used for developing new antibacterial agents.
- Moreover, the cytotoxicity and haemocompatibility results showed excellent biocompatibility of the combinations on human cell line and human serum albumin, respectively, which could potentially improve its utility for the biomedical field.

Keywords Ionic liquid · Melittin · Antibacterial activity · MTT assay · Haemocompatibility

Supplementary Information The online version contains supplementary material available at <https://doi.org/10.1007/s00253-020-10989-y>.

✉ Rajan Patel
rpatel@jmi.ac.in

¹ Biophysical Chemistry Laboratory, Centre for Interdisciplinary Research in Basic Sciences, Jamia Millia Islamia, New Delhi 110025, India

² Department of Zoology, College of Science, King Saud University, P.O. Box 2455, Riyadh 11451, Saudi Arabia

³ Doping Research Chair, Department of Zoology, College of Science, King Saud University, Riyadh 11451, Kingdom of Saudi Arabia

⁴ Department of Bioscience, Jamia Millia Islamia, New Delhi 110025, India

Introduction

The World Health Organization (WHO) report published in 2019 calls for urgent action to avert the antimicrobial resistance crisis. About 700,000 deaths due to drug-resistance diseases take place each year as per the recent WHO report (Organization WH 2019). Bacterial resistance to multiple conventional antimicrobial agents has become a significant global public health threat. Rising antibiotic resistance is seriously threatening the vast medical advancements over the past 70 years (Chemical 2014; Payne 2008; Spellberg et al. 2013). Bacteria acquire innate or intrinsic resistance to conventional drugs due to various biological or climatic changes in the environment (Khameneh et al. 2016). Besides, exponential growth in the bacterial resistance towards antibiotics is due

to the intensive cliché of antibiotics in human medication or an environment comprising agriculture and aquaculture (Hughes and Karlén 2014). Bacterial resistance against conventional antibiotics in hospitals suppresses the immunity of the patients resulting in ineffective treatment of infections (Nascimento et al. 2000; WHO AR 2014). Hence, there is an urgent need for an effective alternative to the antibacterial drug.

Antimicrobial peptides (AMPs) because of their promising and effective antibacterial property against a broad-spectrum microorganism represent promising alternative therapeutic agents over the conventional antibiotics (Regmi et al. 2017). In general, AMPs are known for targeting cell membranes, and the tendency to disrupt the bacterial membrane contributes towards the antimicrobial activity of AMPs. Previously, several studies showed that the combination of the short and synthetic cationic peptide with conventional antibacterial drugs transcends the antibacterial activity which helps to combat the evolution of resistance in bacteria (Maisetta et al. 2009) (Regmi et al. 2017). On the other hand, the combinations of the peptide with antibiotics minimize the noxious effect in the course of the medical procedure involved in the treatment of severe infections caused by microorganisms. Various groups of researchers showed the combined effect of other peptides and drugs on the bacterium and concluded with the same results (Khara et al. 2014). A collaborative effect of peptides and conventional antibacterial drugs may conceivably ameliorate the efficacy of antibacterial agents against several bacterial infections which may intercept the evolution of new resistance against peptide and antibacterial drugs (Akbari et al. 2019). The unique feature of AMPs containing tryptophane (Trp) as one of its residues helps them to bind with the cell membrane via various intermolecular interactions such as hydrogen bond and electrostatic interactions, with the interfacial region of the cell membrane showing more antimicrobial potency of AMP (Khawam and Flanagan 2006). Trp residue in AMP displays indestructible membrane-disruptive activity, and this feature provides Trp-containing peptides with the unique capability to link with the interfacial region of the cell membranes for their good antibacterial activity as compared to AMPs without Trp residue (Khawam and Flanagan 2006).

Therefore, as Trp-containing AMPs show enhanced antibacterial activity, here, we have chosen a cationic peptide, melittin (MEL), as a cationic short peptide that has one Trp (amino acid) as an antibiotic. MEL isolated from *bee venom* displays strong lytic activity against prokaryotic and eukaryotic cells. The action mechanism of MEL involves the pore formation into cells membrane through permeabilization which leads to leakage of cytoplasmic content and finally cell death (Akbari et al. 2019). The second antibiotic we selected was pyrrolidinium-based ionic liquids (ILs) (Zhang et al. 2016a) (Qin et al. 2017). Recently, ionic liquids (ILs) emerge as good antimicrobials agents (Garcia et al. 2013). Despite having wonderful characteristic features, ILs possess some

toxicity features which limit their use in pharmaceutical industries. Therefore, we have synthesized pyrrole-based ILs as previously reported pyrrolidinium-based ILs to possess lesser toxicity as compared to imidazolium, ammonium-based ILs (Qin et al. 2017). ILs possessing versatile characteristic such as low vapour pressure, low melting point, and tuneable nature have gained the interest of researchers to use them in various fields such as drug delivery (Wani et al. 2019), organic solvent, biomedical field, and pharmaceutical industry (Maurya et al. 2019).

Previously, we have synthesized pyrrolidinium-based ILs containing bis(trifluoromethane)sulfonyl imide, $((\text{CF}_3\text{SO}_2)_2\text{N}^-)$ as a counter ion and N-alkyl substituted pyrrole ring as a cation moiety. The study showed a remarkable improvement in the antibacterial activity of melittin in the presence of ILs containing longer chain length (Saraswat et al. 2020). Therefore, in search of a better, cost-effective, and efficient therapeutic agent, we focused our study to further find some more combinations of antibacterial activity of MEL with pyrrolidinium-based ILs which may furnish us with antibacterial agents that might show the best antibacterial activity. Hence, we have synthesized a range of pyrrolidinium-based ILs having N-alkyl substituted pyrrole ring as a cation moiety and Br^- as a counter ion and accessed the effect of ILs on the antibacterial activity of MEL against a couple of microorganisms, *E. coli* and *S. Aureus*, thus creating a more effective approach for the treatment of multidrug resistance. To the best of our knowledge, the present combination has not been used earlier as a potential candidate for the treatment of bacterial resistance.

Materials and methods

Materials

Melittin (purity $\geq 65\%$), pyrene (purity $\geq 99\%$), resazurin, and Luria Bertani Broth (LBB) were obtained from Sigma Aldrich, USA. 1-Methylpyrrolidine, bromoalkanes (1-bromobutane, 1-bromohexane, 1-bromooctane, 1-bromodecane, 1-bromododecane), ethyl acetate, ethanol, CDCl_3 , and acetone of analytical grade were used and were purchased from MERK. Quality control strains, *Escherichia coli* (MTCC 40), and *Staphylococcus aureus* (MTCC 87) were purchased from the microbial-type culture collection and gene bank (MTCC), CSIR-Institute of Microbial Technology, Chandigarh, India. Milli-Q water was used throughout the experiments.

Bacterial strains

LBB media was employed for a culture of microorganisms, *E. coli* and *S. aureus*. The culture was freshly grown at 37°C up to the log phase under an aerobic condition for 16–18 h. The concentration of the bacterial inoculums was determined

by measuring the optical density (OD_{600}) using an Analytikjena 210 (Germany) spectrophotometer. The culture of $OD_{600} = 0.5$ for each microorganism was used to determine the antibacterial efficacy of the synthesized ILs and their effect on the antibacterial property of melittin (an antimicrobial peptide). The final working concentration of the bacterial inoculum was adjusted to 10^6 – 10^5 CFU/mL.

Preparation of testing reagent

Resazurin (dye) was used to evaluate the minimum inhibition concentration (MIC) values of the individual compounds. The solution of resazurin (15%) was prepared by dissolving 0.015 g in distilled water. The solution was vortexed and was filtered using a 0.22- μ m filter. The solution of resazurin was kept at 4 °C and was stored for its use maximum for 4 weeks.

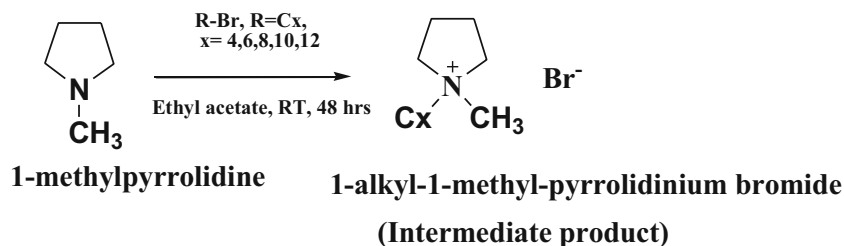
Synthesis of pyrrolidinium based-ILs [Pyr C_x] Br^- ($x = 4, 6, 8, 10, 12$)

IL N-alkyl-N-methylpyrrolidinium bromide was synthesized in our laboratory using a route as described earlier (Qin et al. 2017; Saraswat et al. 2020). To prepare reaction mixture, bromoalkane (butylbromide, hexylbromide, octylbromide, decylbromide, and dodecylbromide) (5.48 g, 0.04 mol) were mixed with N-methylpyrrolidine (3.4 g, 0.04 mol). Ethyl acetate (15 mL) was added to the reaction mixture in round bottom flask as shown in Scheme 1. The reaction mixture was refluxed and stirred continuously and refluxed for 48 h. The course of the reaction was monitored using thin-layer chromatography (TLC) in which TLC plate was visualized under UV (254 nm) light. After refluxing, the obtained ILs were thoroughly washed with ethyl acetate. The solvent was evaporated and the obtained product was kept under high vacuum at an elevated temperature of about 60–70 °C to remove moisture content if any.

Structural characterization

1H nuclear magnetic resonance (NMR) spectra were recorded on Bruker Avance (Delta) operating at 400 MHz, and ^{13}C NMR spectra were recorded with a spectrometer (Delta) operating at 100 MHz. The Fourier transform infrared transform

Scheme 1 Scheme of synthesis of pyrrolidinium-based ILs with Br^- as the counter ion



(FT-IR) spectra were recorded on Bruker tensor 37 FT-IR spectrophotometer in the IR range of 400–4000 cm^{-1} and mass spectra for each synthesized IL were recorded on LC-MS/MS (water), Xevo TDQ, ACQUITY UPLC-H PLUS in the range of 150–700 m/e.

Determination of surface-active parameters of ILs

The surface-active behaviour of newly synthesized pyrrolidinium-based ILs were determined using surface tensiometry and pyrene probe fluorescence spectroscopy (the detailed methodology is given in [supplementary material](#)). Surface tension measurement was performed as described previously (Saraswat et al. 2020; Wani et al. 2019). Figure S22(a–e) shows the plot between γ values of each IL against the concentration where inflexion point in the graph signifies the CMC value (Behera and Pandey 2007; Bhat et al. 2019). Various other interfacial parameters such as Γ_{max} , A_{min} , Π_{cmc} , and P were determined, and their respective values are given in Table S1. The critical micellar concentration (CMC) values of ILs were further confirmed using pyrene probe fluorescence spectroscopy as described earlier (Wani et al. 2019). Figure S23(a–e) represents the fluorescence spectra of pyrene (dilute solution of concentration 1×10^{-6} mol L^{-1}) in the absence and presence of a varied concentration of synthesized ILs (the detailed methodology is given in [supplementary material](#), Fig. S24(a–e)).

Cytotoxicity

The synthesized ILs were screened for their toxicity effect on normal cell line human embryonic kidney (HEK-293) cell line using MTT assay. The cell line, HEK-293, was precured from the National Centre for Cell Science (NCCS), Pune, India. The procedure involved the 10,000 cells/well was grown into the flat-bottom 96-well plates (150 μL /well) in triplicates, allowed to attach and grow. Fresh culture of cells was prepared in T-75 culture flask in Dulbecco's Modified Eagle Medium (DMEM Himedia) containing 10% foetal bovine serum, and penicillium/streptomycin (Himedia), at 37 °C and 5% CO_2 in a humidified chamber (Nuair CO_2 incubator, USA), and the incubation of 24 h was given to the sample. Subsequently, the prepared set of the sample in the plate was treated with various concentrations of the synthesized ILs

ranging from 9.3 to 300 μM . Later, after 48 h of treatment, the medium was removed and cells were incubated with 20 μL of MTT (5 mg/ml in PBS) in fresh medium for 4 h at 37 °C. Solubilization of formazan crystals in DMSO (150 μL /well) was done which was formed by mitochondrial reduction of MTT, and quantification of results was done after an incubation period of 15 min by recording the absorbance at 540 nm on the iMark Microplate Reader (Bio-Rad). The percentage of cell viability was calculated as a fraction of control by using Eq. 1 (Maurya et al. 2019).

$$\% \text{cell viability} = \frac{\text{OD sample mean}}{\text{OD control mean}} \times 100 \quad (1)$$

Antibacterial Activity

Minimum inhibition concentration determination (MIC)

Microbiological toxicity of synthesized ILs against *E. coli* and *S. aureus* was assessed through the determination of MIC values by two-fold serial dilution method according to Clinical and Laboratory Standards Institute guidelines (CLSI) (Clinical, Institute LS 2012). MEL and ILs were gradiently diluted with LBB row-wise into the 96-well plate against *E. coli* and *S. aureus*. The final concentration range for MEL was from 5 to 0.03 μM , whereas for ILs [Pyr C₄]Br⁻, 480 to 0.23 mM, [Pyr C₆]Br⁻ (from 160 to 0.10 mM), [Pyr C₈]Br⁻ (from 14.88 to 0.007 mM), [Pyr C₁₀]Br⁻ (from 4.32 to 0.002 mM), Pyr C₁₂]Br⁻ (from 0.31 to 0.003 mM). After dilution, 10 μL of bacterial inoculums was added including growth control (GC) (broth with inoculums) except for sterile control (SC) (broth without inoculums). The working concentration of inoculum was adjusted to 10⁶–10⁵ CFU/mL. The plate prepared was subjected to incubation at 37 °C for 16–18 h in an orbital shaker. After incubation, 10 μL of 15% solution of resazurin dye was added to each well in 96-well plate. Again, incubation was given to the plate for another 2–4 h for the observation of colour change. After complete incubation, well with no colour change (blue colour of resazurin remained unchanged) before a complete change of colour (blue colour of resazurin was changed to pink) was recorded as the MIC value of the corresponding compound.

Biological activity of MEL in presence of ILs

The antibacterial activity of MEL was accessed in the presence of a range of synthesized ILs as previously reported (Omoya and Ajayi 2016). The experimental procedure includes the two-fold serial dilution of 10 μM MEL along the column in 96-well plate ranging from 5 to 0.03 μM for microorganisms, *E. coli* and *S. aureus*. The selected concentration of each ILs was added to plate; [Pyr C₄]Br⁻ (20 μM , 50

μM , 100 μM , 200 μM , 250 μM) was added vertically in columns 2–6. Subsequently, the same experimental procedure was followed for [Pyr C₆]Br⁻ (10 μM , 50 μM , 100 μM , 200 μM , 250 μM), [Pyr C₈]Br⁻ (5 μM , 10 μM , 50 μM , 100 μM , 200 μM), [Pyr C₁₀]Br⁻ (5 μM , 10 μM , 20 μM , 50 μM , 100 μM), and [Pyr C₁₂]Br⁻ (1 μM , 2 μM , 5 μM , 10 μM , 20 μM). Lastly, 10 μL of inoculums whose concentration was adjusted to 10⁶–10⁵ CFU/mL added to each well except SC. The plate was incubated at 37 °C for 16–18 h. After complete incubation, the quantification of results was done by recording the optical density (OD) at 600 nm which was recorded on iMark Microplate Reader (Bio-Rad) for each plate. Each test was performed in the triplicate set.

Impact of ILs on MEL's secondary structure

The changes in the secondary structure of MEL induced by ILs were monitored in the far-UV region (200–250 nm) using a quartz cuvette of the path length of 0.1 cm (Patel et al. 2018). The ellipticity value at wavelengths 222 nm and 207 nm were used to calculate the *R* value using Eq. 2 (Morrisett et al. 1973; Zhang et al. 2016b).

$$R = \frac{[\theta]_{222}}{[\theta]_{207}} \quad (2)$$

where $[\theta]_{207}$ and $[\theta]_{222}$ are the experimentally observed absolute mean residue ellipticity at 207 nm and 222 nm, respectively.

Haemocompatibility assay

For haemocompatibility observation of IL-MEL compositions, steady-state fluorescence, absorption, and CD spectroscopy were employed. Samples prepared for haemocompatibility assay includes 5 μM HSA alone and in the presence of 10 μM MEL. A separate set of samples was prepared which contained MEL, HSA, and ILs where ILs, [Pyr C₄]Br⁻ (50 μM); [Pyr C₆]Br⁻ (25 μM); [Pyr C₈]Br⁻ (20 μM); and [Pyr C₁₀]Br⁻ (10 μM); [Pyr C₁₂]Br⁻ (5 μM) were varied and kept the concentration of MEL and HSA constant in each sample set. All samples were incubated at 300 K for 30 min. The fluorescence spectra of each sample were obtained at 298 K on a fluorescence spectrophotometer (Cary Eclipse spectrophotometer (Varian, USA)) fitted with 150 W xenon lamp. The temperature of the sample holder was controlled using a Peltier control temperature device. The sample was excited at 280 nm and emission was recorded between 290 and 500 nm keeping the slit width 5 nm constant for all the spectral scans. Absorption spectra of the same set of samples were obtained between 200 and 400 nm with a slit width of 1 nm on a UV-Vis spectrophotometer (Analytik Jena Specord-250 spectrophotometer, Germany) and kept the slit width 1 nm constant of all spectral

scans. Additionally, far-UV-CD spectra of the same set of samples were recorded with a quartz cuvette of 0.1-cm path length on a spectropolarimeter (Jasco-715 spectropolarimeter) equipped with a microcomputer at 298 K. The spectropolarimeter was calibrated using D-10-camphorsulfonic acid. The temperature of the sample holder was maintained using a water bath with an accuracy of ± 0.1 °C to the spectropolarimeter.

Binding study

The effect of synthesized ILs on the conformation of MEL was studied using various spectroscopic and molecular docking (MD) methods. Initially, MD was employed to determine the binding mode and binding site on MEL. MD was performed using AutoDock 1.5.6 software. After docking, the conformations were ranked and placed according to their increasing binding energy obtained from molecular docking. Amongst all five ILs, the best combination of MEL-ILs was selected based on the highest binding energy. Further, the interaction study of MEL with [Pyr C₁₂]Br⁻ (IL with the highest binding energy obtained from MD) was studied using various spectroscopic techniques, viz. fluorescence, UV-visible, and CD spectroscopy.

The fluorescence spectra of MEL (5 μ M) in Tris buffer (10 mM, 7.2 pH) alone and in the presence of a varied concentration of [Pyr C₁₂]Br⁻ (1.42 μ M to 20.97 μ M) at 298 K, 303 K, 308 K, and 313 K was recorded on the same instrument as described earlier (Gbaj 2018; Patel et al. 2015) (the detailed methodology is given in [supplementary materials](#)). The UV spectra of MEL (5 μ M) alone and in the presence of a varied concentration of [Pyr C₁₂]Br⁻ (from 1.42 to 20.97 μ M) was recorded using the same UV spectrophotometer as earlier described at 298 K. For recording the absorbance, quartz cuvette of 1-cm path length was used and the spectra were recorded in the range of 200–400 nm (Patel et al. 2015; Sharma et al. 2017).

Results

Structural characterization

The chemical structure of synthesized ILs, 1-butyl-1-methylpyrrolidinium bromide [Pyr C₄]Br⁻, 1-hexyl-1-methylpyrrolidinium bromide [Pyr C₆]Br⁻, 1-methyl-1-octylpyrrolidinium bromide [Pyr C₈]Br⁻, 1-decyl-1-methylpyrrolidinium bromide [Pyr C₁₀]Br⁻, and 1-dodecyl-1-methylpyrrolidinium bromide [Pyr C₁₂]Br⁻ (shown in Fig. S21), were synthesized in our laboratory using a route as shown in Scheme 1. ¹H NMR, ¹³C NMR in CDCl₃/DMSO-d₆ (solvents), FT-IR, and mass spectra confirmed the chemical structure of the synthesized compounds. Chemical shift values for protons and carbons are reported in ppm.

Tetramethylsilane (TMS) was used as a reference solvent. The NMR data are reported as follows: chemical shift, multiplicity (s = singlet, br s = broad singlet, d = doublet, t = triplet, q = quartet, m = multiplet, dd = doublet of doublet), coupling constants in Hertz and integration. TLC analysis was performed on commercially prepared F-254 silica gel plates and visualized under UV irradiation. To further confirm the structure, liquid chromatography-mass spectroscopy (LCMS) mass spectra and Fourier transform infrared FT-IR was done.

1. *1-Butyl-1-methylpyrrolidin-1-ium bromide*, [Pyr C₄]Br⁻. The product was obtained as a brown oil. ¹H NMR (400 MHz, CDCl₃) δ 3.71–3.64 (m, 4H), 3.52–3.48 (m, 2H), 3.13 (s, 3H), 2.62 (s, 1H), 2.17–2.15 (m, 4H), 1.67–1.59 (m, 2H), 1.35–1.25 (m, 2H), 0.84 (t, J = 7.4 Hz, 3H); ¹³C NMR (100 MHz, CDCl₃) δ 64.5, 64.0, 48.7, 25.9, 21.7, 19.7, 13.7; FT-IR (4000–400 cm⁻¹) 2998 cm⁻¹ [$\nu_{(N-C)}$], 2915 cm⁻¹ [$\nu_{(C-H)}$ (stretch)], 1485 cm⁻¹ [$\nu_{(CH_2)}$], 1192 cm⁻¹ [$\nu_{(C-C)}$ (Bend)], 888 cm⁻¹ [$\nu_{(C-H)}$ (Bend)], 3320 cm⁻¹ is due to absorbed moisture. LCMS (ESI) [M + H]⁺ calculated for [C₉H₂₀BrN] 221.0779, found 222.2706. (detailed spectra is given in Fig. S1-4)

2. *1-Hexyl-1-methylpyrrolidin-1-ium bromide*, [Pyr C₆]Br⁻. The product was obtained as brown oil. ¹H NMR (400 MHz, CDCl₃) δ 3.72–3.61 (m, 4H), 3.50–3.46 (m, 2H), 3.11 (s, 3H), 2.70 (s, 1H), 2.20–2.17 (m, 4H), 1.69–1.61 (m, 2H), 1.30–1.23 (m, 2H), 1.22–1.15 (m, 3H), 0.75 (t, J = 7.1 Hz, 3H); ¹³C NMR (100 MHz, CDCl₃) δ 64.5, 64.3, 48.7, 31.3, 26.1, 24.0, 22.4, 21.7, 13.9; FT-IR (4000–400 cm⁻¹) 2998 cm⁻¹ [$\nu_{(N-C)}$], 2915 cm⁻¹ [$\nu_{(C-H)}$ (stretch)], 1485 cm⁻¹ [$\nu_{(CH_2)}$], 1192 cm⁻¹ [$\nu_{(C-C)}$ (Bend)], 888 cm⁻¹ [$\nu_{(C-H)}$ (Bend)], 3320 cm⁻¹ is due to absorbed moisture. LCMS (ESI) [M + H]⁺ + calculated for [C₁₁H₂₄BrN] 249.1092, found 250.00 (detailed spectra is given in Fig. S5-8).

3. *1-Methyl-1-octylpyrrolidin-1-ium bromide*, [Pyr C₈]Br⁻. The product was obtained as a brown oil. ¹H NMR (400 MHz, CDCl₃) δ 3.80–3.68 (m, 4H), 3.56–3.52 (m, 2H), 3.21 (s, 3H), 2.56 (s, 1H), 2.24 (s, 4H), 1.75–1.67 (m, 2H), 1.35–1.19 (m, 9H), 0.81 (t, J = 7.1 Hz, 3H); ¹³C NMR (100 MHz, CDCl₃) δ 64.5, 64.3, 48.8, 31.7, 29.2, 29.1, 26.4, 24.1, 22.6, 21.7, 14.1; FT-IR (4000–400 cm⁻¹) 2998 cm⁻¹ [$\nu_{(N-C)}$], 2915 cm⁻¹ [$\nu_{(C-H)}$ (stretch)], 1485 cm⁻¹ [$\nu_{(CH_2)}$], 1192 cm⁻¹ [$\nu_{(C-C)}$ (Bend)], 888 cm⁻¹ [$\nu_{(C-H)}$ (Bend)], 3320 cm⁻¹ is due to absorbed moisture. LCMS (ESI) [M + H]⁺ + calculated for [C₁₃H₂₈BrN] 277.1405, found 278.3205 (detailed spectra are given in Fig. S9-12).

4. *1-Decyl-1-methylpyrrolidin-1-ium bromide*, [Pyr C₁₀]Br⁻. The product was obtained as a brown oil. ¹H NMR (400 MHz, CDCl₃) δ 3.68–3.56 (m, 4H), 3.44–3.40 (m, 2H), 3.10 (s, 3H), 2.87–2.83 (m, 1H), 2.18–2.10 (m, 4H), 1.64–1.56 (m, 2H), 1.25–1.19 (m, 3H), 1.13–1.10 (m, 10H), 0.70 (t, J = 6.8 Hz, 3H) ¹³C NMR (100 MHz, CDCl₃) δ 64.5, 64.2, 48.7, 31.8, 29.4, 29.4, 29.2, 26.4, 24.1, 22.6, 21.7, 14.1; FT-IR

(4000–400 cm^{-1}) 2998 cm^{-1} [$\nu_{(N-C)}$], 2915 cm^{-1} [$\nu_{(C-H)}$ (*stretch*)], 1485 cm^{-1} [$\nu_{(CH_2)}$], 1192 cm^{-1} [$\nu_{(C-C)}$ (*Bend*)], 888 cm^{-1} [$\nu_{(C-H)}$ (*Bend*)], 3320 cm^{-1} is due to absorbed moisture. LCMS (ESI) [M + H]⁺ calculated for [C₁₅H₃₂BrN] 305.1718, found 305.2522 (detailed spectra is given in Fig. S13–16)

5. *1-Dodecyl-1-methylpyrrolidin-1-ium bromide*, [Pyr C₁₂]Br⁺. The product was obtained as a brown oil. ¹H NMR (400 MHz, CDCl₃) δ 3.52–3.46 (m, 4H), 3.28–3.24 (m, 2H), 3.01 (s, 3H), 2.25–2.23 (m, 3H), 1.75–1.63 (m, 2H), 1.32–1.24 (m, 19H), 0.86 (t, $J = 7.2$ Hz, 3H). ¹³C NMR (100 MHz, CDCl₃) δ 64.8, 64.5, 48.5, 48.2, 31.8, 29.5, 29.4, 29.3, 28.9, 26.1, 23.8, 22.6, 21.4, 14.1; FT-IR (4000–400 cm^{-1}) 2998 cm^{-1} [$\nu_{(N-C)}$], 2915 cm^{-1} [$\nu_{(C-H)}$ (*stretch*)], 1485 cm^{-1} [$\nu_{(CH_2)}$], 1192 cm^{-1} [$\nu_{(C-C)}$ (*Bend*)], 888 cm^{-1} [$\nu_{(C-H)}$ (*Bend*)], 3320 cm^{-1} is due to absorbed moisture. LCMS (ESI) [M + H]⁺ calculated for [C₁₇H₃₆BrN] 333.2031, found 333.3132 (detailed spectra is given in Fig. S17–20).

Determination of surface-active parameters of ILs

The optimum biological effect of ILs is attributed to various surface-active properties of ILs, viz. adsorption, hydrophobicity, micellization, migration to the cell wall, solubility, etc. (Saraswat et al. 2020). The variability in the antimicrobial efficacy of ILs is associated with a bunch of various surface-active parameters such as critical micelle concentration (CMC), the minimum area per molecule (A_{min}), surface excess concentration (Γ_{max}), and an index of surface reduction (Π_{cmc}), which in terms of numerical data describes the physicochemical behaviour of ILs as reported by several research groups (Garcia et al. 2013; Garcia et al. 2017; Saraswat et al. 2020). Therefore, to optimize the biological effect of synthesized ILs, the surface activity of synthesized pyrrole-based ILs in aqueous medium was studied using surface tension data. The details are given in [supplementary material](#).

The surface tension, γ , was recorded and was plotted against the concentration of ILs in the water at 298 K as shown in Fig. S22(a–e). CMC, A_{min} , Γ_{max} , and P values were determined using the surface tension data. The obtained CMC values and other parameters are listed in Table S1. The presence of varied carbon chain length at N atom in cation significantly showed variation in the antibacterial activity which was elucidated based on numerical data of CMC, A_{min} , Γ_{max} , the free energy of adsorption (ΔG_{ads}), and standard free energy for micellization (ΔG_{mic}) shown in Table S1. From Table S1, a higher magnitude of ΔG_{ads} as compared to ΔG_{mic} indicate that the adsorption is a most favoured process than micellization at the air-water interface. Also, the value of ΔG_{ads} has increased with the elongation of alkyl chain length which further advocates the increasing spontaneity of higher analogs to get adsorb on the surface (details are given in

supporting information). The results obtained from tensiometry suggest that the variation in the alkyl chain at N-atom in the pyrrole ring can modify not only the micellization behaviour of ILs but also lead to functional differences in both efficacy and antibacterial activity of ILs.

Cytotoxicity

The cell toxicity of synthesized ILs was administered on HEK 293 cell line, using various concentrations (9.3–300 μM). Good response in terms of cell viability (value ranges between 80 and 95%) was shown by all ILs at lower concentrations up to 150 μM . The cell viability at a lower concentration of all the five ILs showed almost similar value, while at higher concentrations there was a decrease seen in the cell viability at around 150–300 μM for [Pyr C₁₂]Br⁺ (value ranges from 85 to 90%) as shown in Fig. 1(a). This suggests that all five synthesized ILs were non-toxic to normal HEK cell line at lower concentration ranging up to 150 μM . These results were compared with the data already been reported and were found that the synthesized pyrrolidinium-based ILs possess lesser toxicity as compared to the reported imidazolium-, pyridinium-, and ammonium-based ILs (Qin et al. 2017). This finding was further used in in vitro studies to further choose the concentration range which may induce lesser damage to the human cell and could result in better antibacterial property.

Antibacterial activity

MIC determination

The synthesized ILs were screened for their antibacterial property by investigating minimum inhibition concentration (MIC) against using *E. coli* and *S. aureus*. MIC is defined as the minimum concentration required for the inhibition of 50% of the total bacterial growth after 24 h. The obtained MIC values are summarized in Fig. 1(b). The MIC values suggest that ILs with longer alkyl chain are more susceptible to *E. coli* and *S. aureus* as compared to ILs with shorter alkyl chain length, hence showing the larger MIC value. The structural similarity of pyrrolidinium-based ILs with imidazolium-based ILs containing quaternary ammonium cation makes them also a good candidate as an antibacterial agent. Imidazolium-based ILs are known for their activity towards membrane at the target site mainly at the cytoplasmic membrane. ILs are the amphiphilic molecules that have a tendency of impairment with negatively charged entity mainly the phosphate group present in a cell membrane through electrostatic forces which favours the adsorption onto the cell through hydrophobic-hydrophobic interaction. Hydrophobic-hydrophobic interaction allows the insertion of ILs into the cell membrane via pore formation (poration) leading to the rupturing of the cell

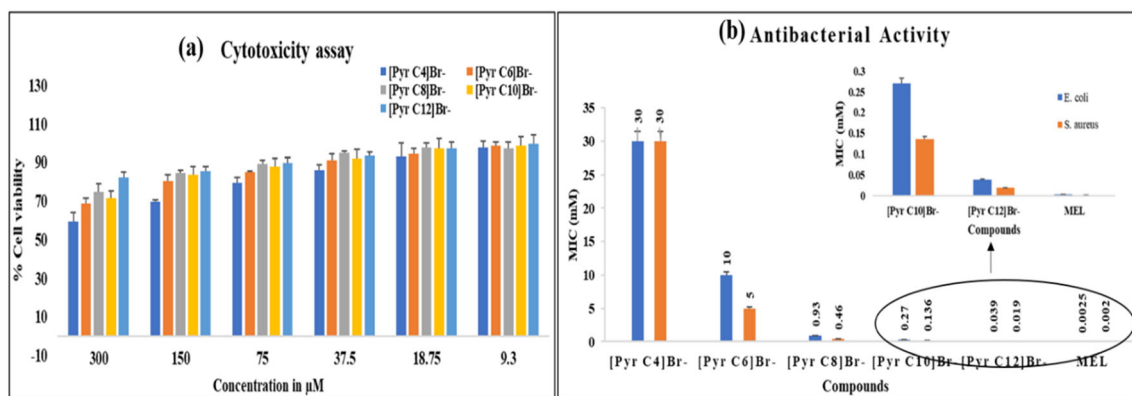


Fig. 1 (a) Cytotoxicity assay of synthesized pyrrole-based ILs with Br⁻ as counter ion at various concentration. (b) Showing the MIC values of [Pyr C₄]Br⁻, [Pyr C₆]Br⁻, [Pyr C₈]Br⁻, [Pyr C₁₀]Br⁻, [Pyr C₁₂]Br⁻, and MEL against *E. coli* and *S. aureus*

wall with leakage of electrolyte out of the cell and ultimately to cell death (Florio et al. 2019).

Mean MIC values of homologues of pyrrolidinium-based ILs against a couple of microorganisms are listed in Fig. 1(b) which show the decreasing trend with the increasing carbon atoms in the chain as previously reported for various surface-active ILs (Garcia et al. 2017). The obtained MIC values for each IL and MEL are listed in Fig. 1(b) which clearly show that the MIC values of ILs against *E. coli* (*Gram-negative*) were greater as compared to the MIC values against *S. aureus* (*Gram-positive*). The difference in susceptibility towards the action of the pyrrolidinium ILs against *E. coli* and *S. aureus* can be deduced based on the structural difference between *Gram-negative* and *Gram-positive* bacteria cells. Structurally, *Gram-positive* bacteria comprise a much thicker porous membrane of about 20–70 nm made up of peptidoglycan layer interlinked with each other by a negatively charged teichoic acid which is responsible for its porosity. On the contrary, the *Gram-negative* bacterial membrane comprises two layers: the outer layer being negatively charged whose thickness is about 7–8 nm and is made up of lipopolysaccharides, whereas the inner membrane is relatively thin (2–7 nm) which is made up of peptidoglycan (Qin et al. 2017). Therefore, it is supposed that the hydrophobic part of IL is more likely to insert into the porous cell, peptidoglycan membrane resulting in the disruption of the cell membrane and cell death. In the case of *Gram-negative* bacteria, the outer membrane protects the cell from the entry of foreign body such as surfactant molecule which will ultimately disrupt the inner peptidoglycan layer in the cell. In *Gram-positive* bacteria, the outer layer of peptidoglycan may absorb the surfactant molecule by hydrophobic interaction and carry it to the inner cell membrane leading to disruption of the cell wall. Figure 1(b) shows the MIC values of ILs in the form of a bar graph which clearly shows the dependence of alkyl chain length of ILs on microbiological toxicity against clinical microorganism, *E. coli* and *S. aureus*. [Pyr C₁₂]Br⁻ and [Pyr C₁₀]Br⁻ showed the maximum efficacy against both the

microorganism as compared to ILs with smaller alkyl chain lengths.

The biological effect of ILs also depends on the diverse physicochemical properties such as critical micelle concentration, hydrophobicity, adsorption, accumulation at the cell membrane, solubility, and transport in the medium. The maximum surface area (Γ_{max}) and the minimum area (A_{min}) occupied by a single surfactant molecule at the air-water interface obtained from Gibb's adsorption isotherm give an idea about the surface arrangement of surfactant molecules. The greater value of Γ_{max} and a smaller value of A_{min} depict the denser arrangement of molecules at the interface. From Table S1, the value of Γ_{max} increases with increasing the chain length, indicating the increase in the compactness at the interface which was further supported by the A_{min} value. The decreasing value of A_{min} with increasing chain length suggests the increase in the packing of the molecule at the interface due to the decreased repulsive force between the IL molecules that is the ILs with longer chain length forms the more compact monolayers at the interface. For higher homologues, CMC value decreased which indicates that the accumulating concentration of IL at cell membrane becomes less. Further, the free energy of adsorption (ΔG_{ads}^o) for each IL was calculated and is listed in Table S1 which shows the increase with increasing hydrophobic chain length. Also, the value of ΔG_{ads}^o was found to be higher as compared to the value of ΔG_{mic}^o suggesting the favoured adsorption on micellization. Further negative increase in the value of ΔG_{ads}^o with longer chain length shows an increase in the migration rate of higher analogs at the cell membrane (Garcia et al. 2013; Qin et al. 2017). All physicochemical parameters for ILs examined collectively show the highest tendency of ILs with longer alkyl chain length to get adsorbed on the cell membrane and hence show the relative higher antibacterial activity for higher analogs. Apart from this, there are several other factors such as adsorption of ILs on the cell membrane subsequently penetrating the living bacterial cell and altering the permeability of the cell wall which are responsible for their best performance (Garcia et al. 2013).

Biological activity of MEL in presence of ILs

Figures 2, 3, 4, 5, and 6 (a–b) show the effect of various concentrations of each synthesized ILs on the microbial property of MEL in terms of the growth curves. The effect of ILs on the antibacterial activity of MEL was studied by examining the inhibition of *E. coli* and *S. aureus*. The results showed a remarkable decrease in the MIC value of MEL in the presence of ILs specially ILs with longer chain length, viz. [Pyr C₈]Br⁻, [Pyr C₁₀]Br⁻ and [Pyr C₁₂]Br⁻. The MIC value of MEL was found to be 2.50 μM and 2.30 μM against *E. coli* and *S. aureus*, respectively. Figure 2(a) shows the effect of [Pyr C₄]Br⁻ on the MIC value of MEL; it was seen that with increasing concentration of IL in combination with MEL the inhibition of bacterial burden was increased. The combination of 1.24 μM MEL with 250 μM [Pyr C₄]Br⁻ showed the reduction in the bacterial growth when tested against *E. coli*, whereas 50 μM [Pyr C₄]Br⁻ in combination with 1.27 μM MEL was tested against *S. aureus* which is shown in Fig. 2(b). Similarly, a composition of MEL and [Pyr C₆]Br⁻ was tested. The improved MIC values were obtained as compared to the combination of [Pyr C₄]Br⁻ with MEL and MEL alone. The reduction in the bacterial burden was observed in case of 200 μM [Pyr C₆]Br⁻ and 1.22 μM MEL shown in Fig. 3(a) against *E. coli*, whereas 10 μM [Pyr C₆]Br⁻ when combined with 0.61 μM MEL is shown in Fig. 3(b) against *S. aureus*. Yet another, the combination of MEL with [Pyr C₈]Br⁻ was tested which further showed improved results in terms of a decrease in MIC value of MEL. 100 μM solution of [Pyr C₈]Br⁻ with 0.77 μM MEL is shown in Fig. 4(a) against *E. coli*, and 100 μM combination of [Pyr C₈]Br⁻ mixed with 1.25 μM MEL is shown in Fig. 4(b) against *S. aureus*. The fusion of 20 μM [Pyr C₁₀]Br⁻ combined with 0.62 μM MEL against *E. coli* and combination of 20 μM [Pyr C₁₀]Br⁻ with 0.64 μM MEL against *E. coli* and *S. aureus* as shown in Fig. 5(a–b), respectively, shows the much more improved results as compared to the combination tested with ILs having butyl, hexyl, and octyl chain lengths. All synthesized ILs in combination with MEL showed improved results especially with increasing chain length in terms of inhibition of bacterial cells. The best response in terms of the maximum inhibition is shown in Fig. 6(a–b) when susceptible *E. coli* was treated with a combination of 0.52 μM MEL and 10 μM [Pyr C₁₂]Br⁻ and *S. aureus* strains when tested with a combination of 0.63 μM MEL and 10 μM [Pyr C₁₂]Br⁻ for 16–18 h. All combinations are listed in Table 1.

The results obtained from the synergistic study of ILs showed an improved MIC value of MEL against both the strain. Amongst all five ILs, the presence of [Pyr C₈]Br⁻, [Pyr C₁₀]Br⁻ and, [Pyr C₁₂]Br⁻ with MEL showed a remarkable improvement in the MIC value of MEL. The combination of antibiotics is one way to overcome the problem associated with the rising multidrug resistance

Table 1 Showing the best combination of synthesized pyrrolidinium based ILs with MEL

Microorganisms	MIC (μM)		
	MEL Alone	In presence of [Pyr C ₄]Br ⁻	
		50 μM	250 μM
<i>E. coli</i> (MTCC 40)	2.50	-	1.24
<i>S. aureus</i> (MTCC 87)	2.30	1.27	-
Microorganisms	MEL Alone	In presence of [Pyr C ₆]Br ⁻	
		10 μM	250 μM
<i>E. coli</i> (MTCC 40)	2.50	-	1.22
<i>S. aureus</i> (MTCC 87)	2.30	0.61	-
Microorganisms	MEL Alone	In presence of [Pyr C ₈]Br ⁻	
		100 μM	
<i>E. coli</i> (MTCC 40)	2.50	0.77	
<i>S. aureus</i> (MTCC 87)	2.30	0.77	
Microorganisms	MEL Alone	In presence of [Pyr C ₁₀]Br ⁻	
		20 μM	
<i>E. coli</i> (MTCC 40)	2.50	0.62	
<i>S. aureus</i> (MTCC 87)	2.30	0.64	
Microorganisms	MEL Alone	In presence of [Pyr C ₁₂]Br ⁻	
		10 μM	
<i>E. coli</i> (MTCC 40)	2.50	0.52	
<i>S. aureus</i> (MTCC 87)	2.30	0.63	

(MDR) of bacteria. Therefore, we decided to design a combination of peptide and ILs. Since MEL is a natural known antibiotic and that was selected due to its high solubility in water. The second antibacterial agent, we have selected in this study was pyrrolidinium based IL whose biological activity was examined separately. Numerous reasons are there that are responsible for the development of bacterial resistance. One being most generous is the frequent and higher dosage of antibiotics. Therefore, we emphasized to increase the antibacterial potential of MEL in the presence of synthesized ILs. This might reduce the intake of MEL as well as will reduce the risk of resistance development against bacterial strain as well. The best results were obtained in terms of bacterial growth inhibition.

The overuse of antibiotics is a reason for severe problems. The combination approach opens up the floor for the researchers to work in the direction where they may curtail the side effect associated with the prolonged use of antibiotics and their high dosage. The combination of two or more antibiotics is nowadays a recent topic of research amongst the researchers to develop an efficient antibiotic to render the multidrug resistance (MDR) (Issam et al. 2015). The distinctive feature of ILs to get adsorbed on the surface makes them an eligible

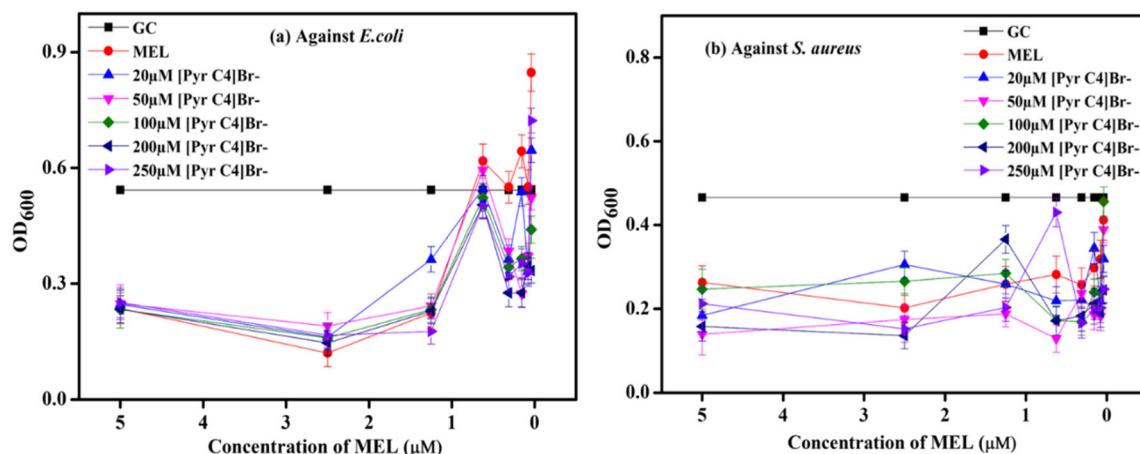


Fig. 2 Showing the effect of [Pyr C₄]Br⁻ concentration on antibacterial activity of MEL against (a) *E. coli* and (b) *S. aureus*

candidate to be used as a substitute compound for the development of combination drug as discussed previously based on the parameters listed in Table S1.

Impact of ILs on MEL's secondary structure

Before going into the application part of the non-covalent conjugate of MEL and synthesized pyrrole-based ILs as an antimicrobial agent, the conformational study was performed using far-UV-CD spectroscopy. The conformational change in the secondary structure of MEL was evaluated in the presence of ILs. The far-UV-CD spectra were recorded to study the effect of ILs on the secondary structure of MEL. The CD spectra of MEL alone and in the presence of ILs were recorded as shown in Fig. 7(a–e). MEL showed a two-negative peak at around 208 and 222 nm which are evidence of α -helical structure; the obtained spectra agrees with the reported spectra (Zhang et al. 2016b). The spectra were used to determine the molar ellipticity ratio, R . In Table S3, the value of R of conjugates was found to be approximately similar to the R -value of pure MEL which demonstrates that alkyl chain attached at

N-position in IL did not affect the secondary structure of the peptide, MEL (Reinhardt et al. 2014).

Haemocompatibility assay

For the clinical application of any antibacterial agent, haemocompatibility is an important aspect to be taken care of; hence, haemocompatibility test was performed on the key component of blood, human serum albumin, (HSA) (a transport protein). HSA plays an important role in biological functions in the body. It maintains the stability of the circulatory system (Patel et al. 2018). Therefore, the interaction of HSA with MEL and MEL-ILs was investigated. Intrinsic fluorophore (tryptophan, tyrosine) in HSA is responsible for the fluorescence signal and is often used to assess the structural change in the protein of any while interacting with ligand (drug, ILs, or other material) (Kumari et al. 2014; Maurya et al. 2016; Patel et al. 2015). Figure 8(a) shows the fluorescence emission spectra of HSA, where a maximum fluorescence intensity was observed at 342 nm wavelength (λ_{max}) which is a signatory peak for the presence of Trp residue in HSA. Further, the fluorescence emission spectra of HSA in

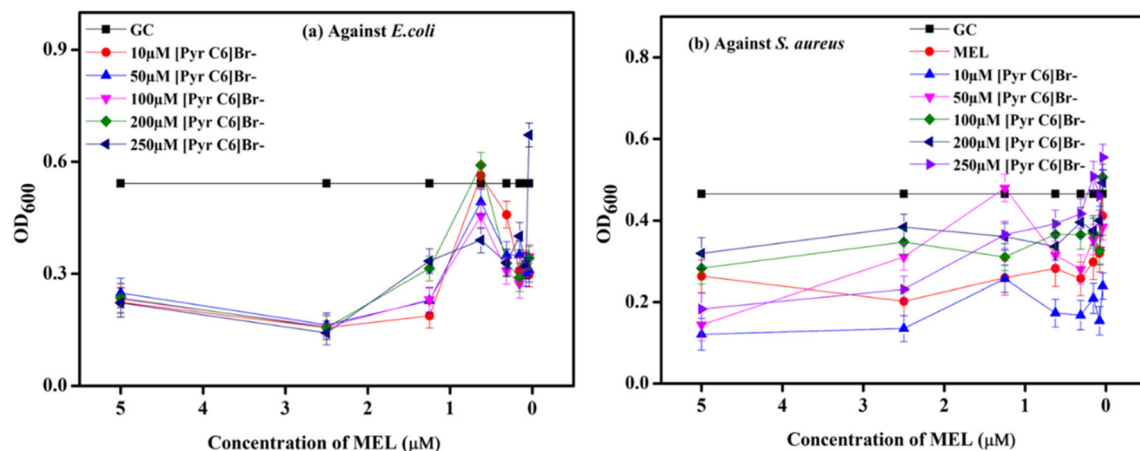


Fig. 3 Showing the effect of [Pyr C₆]Br⁻ concentration on antibacterial activity of MEL against (a) *E. coli* and (b) *S. aureus*

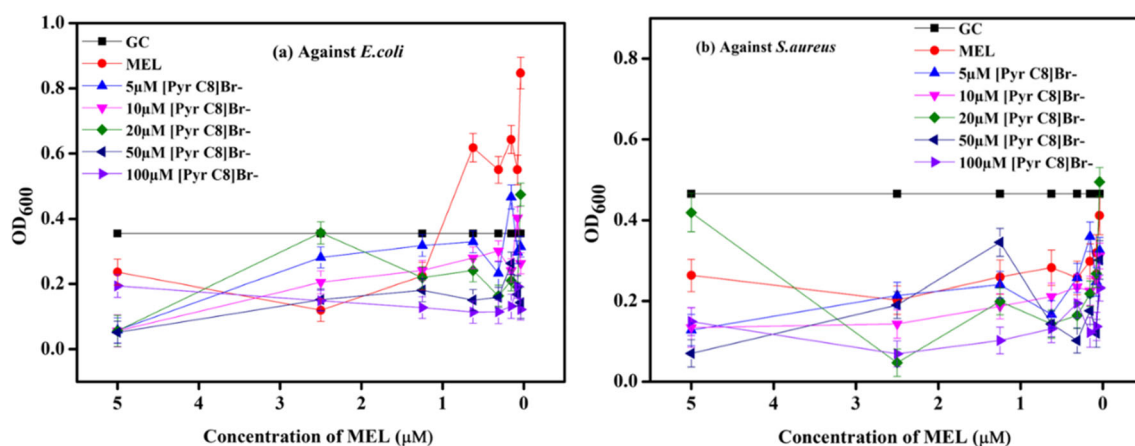


Fig. 4 Showing the effect of [Pyr C₈]Br⁻ concentration on antibacterial activity of MEL against (a) *E. coli* and (b) *S. aureus*

the presence and absence of MEL and its combination with ILs were recorded. Fluorescence emission spectra of HSA in the presence of MEL and its combination with ILs do not show any shift in the λ_{max} value, which reveals that the polarity of Trp remains unchanged in the presence of MEL and its combinations with ILs. However, the fluorescence emission intensity of HSA showed an increase in intensity suggesting the addition of fluorescence intensity of MEL due to the presence of one Trp molecule; however, fluorescence intensity decreased (quenching) with the addition of the conjugate to HSA. This may be due to several mechanisms that occur such as energy transfer, the formation of the complex, and the reaction in excited state and collision. In contrast, the increasing fluorescence intensity of HSA in the presence of MEL may be due to the interaction of MEL with HSA by electrostatic attraction leading to change in the microenvironment of Trp. UV-Vis spectra of the same set of samples were recorded to administer the structural changes and complex formation. The absorption spectra showed the characteristic band for α -helix structure in the 200–240 nm range. Figure 8(b) shows no shift in the UV-Vis absorption band which indicates that the secondary structure of HSA remains unchanged in the presence

of MEL and its conjugates with ILs. To administer any change in the secondary structure, far-UV-CD spectra of the same set samples were also obtained as shown in Fig. 8(c). From Fig. 8(c), the increasing negative ellipticity of HSA in the presence of MEL and its conjugates reveals that MEL, as well as its conjugates, do not disturb the secondary structure of HSA; rather, they stabilize the secondary structure of HSA. The results procured from far-UV-CD spectra were found to be competent with the results obtained from the fluorescence and UV-visible spectroscopy. Therefore, it can be concluded from the above results that the non-covalent conjugate is haemocompatible and can be used for developing therapeutic drugs against which could work efficiently against bacterial resistance.

Binding study

To study the complex formation between MEL and synthesized IL, the binding study was performed. Initially, molecular docking was performed which showed the participation of van der Waal and π -cation interaction between MEL and synthesized ILs. The amino acids involved in van der Waal

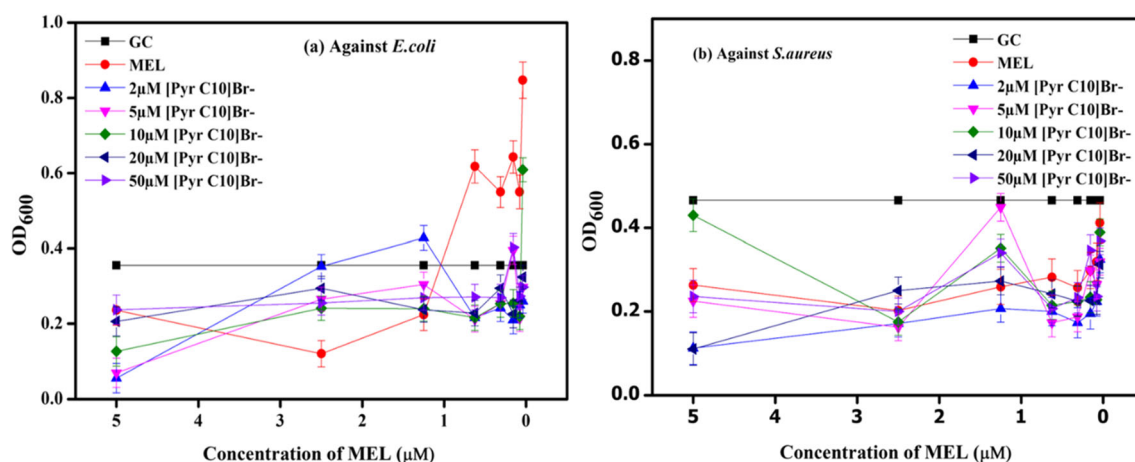


Fig. 5 Showing the effect of [Pyr C₁₀]Br⁻ concentration on antibacterial activity of MEL against (a) *E. coli* and (b) *S. aureus*

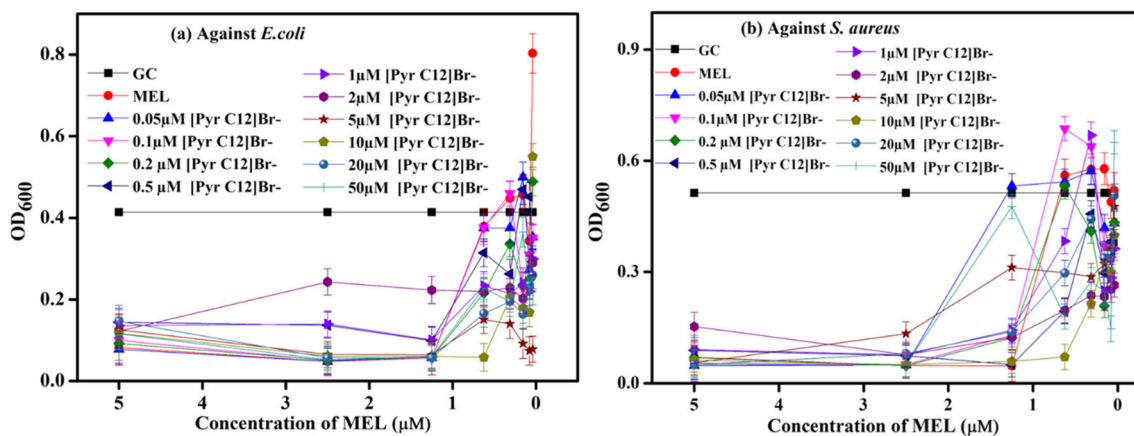


Fig. 6 Showing the effect of [Pyr C₁₂]Br⁻ concentration on antibacterial activity of MEL against (a) *E. coli* and (b) *S. aureus*

interactions were Lys23, Arg22, and Ser18, whereas Trp19 was involved in π -cation interaction. Obtained Gibb's free energy of complexation is listed in Table S2. From Table S2, the value of Gibb's free energy indicates that the complex formation between the MEL and ILs was spontaneous. The increasing negative magnitude of free energy with increasing alkyl chain length in ILs implies the increasing spontaneity of the complex formation with higher analogs. Based on Gibb's free energy obtained from molecular docking, the ILs were ranked with the most possible stable conformation. Figure S25(a–b) shows the most stable and favourable three-dimensional and two-dimensional depiction of the conformation of MEL-[Pyr C₁₂]Br⁻. Further, based on the mathematical value (Table S2) and stability, the most favourable IL, [Pyr C₁₂]Br⁻, was selected for binding study with MEL. Fluorescence and UV-Vis spectroscopy was employed to study the complex formation and feasibility of complex formation between MEL and [Pyr C₁₂]Br⁻ (Maurya et al. 2016; Patel et al. 2015). Firstly, fluorescence measurement was done which showed a progressive decrease in the fluorescence intensity (Fig. S26(a)) of MEL at λ_{max} 353 nm on the addition of the increasing concentration of [Pyr C₁₂]Br⁻. Figure S26(b) shows the plot between F_0/F and concentration of [Pyr C₁₂]Br⁻, where slope corresponds to Stern-Volmer constant, K_{sv} . The K_{sv} value was found to be decreasing with increasing temperature which suggests the process of quenching was static. Further, binding parameters such as binding constant (K_b) and the number of binding sites (n) (details are given in supporting information, Fig. S27. (a)) were evaluated. The values are listed in Table 2. The value of K_b suggests the strong binding between [Pyr C₁₂]Br⁻ with MEL. Besides, the value of n indicates 1:1 binding occurring amongst MEL and [Pyr C₁₂]Br⁻. On increasing the temperature, the value of K_b decreased suggests that at the higher temperature the complex destabilized. The thermodynamic parameters such as free energy change (ΔG), the enthalpy change (ΔH), and entropy change (ΔS) were also calculated which suggests the involvement of van der Waal interaction

and hydrogen bonding in the complex formation (Ross and Subramanian 1981) (detailed explanation is given in supporting information, Fig. S27. (b)). Moreover, the UV-Vis spectrum was obtained to collect insightful information about the complex formation between the MEL and [Pyr C₁₂]Br⁻. Figure S28(a) shows the absorption spectra of MEL alone and in the presence of [Pyr C₁₂]Br⁻. The maximum absorption of MEL was obtained around 273 nm. The K_b was also determined which is in good agreement with fluorescence results (details are given in supporting information)

Discussion

The combination of two or more antibiotic drugs is one way to combat bacterial resistance and is termed as 'combination therapy'. The emergence to develop new antibacterial agents has been a current topic of concern for the researchers where combination therapy had been considered as an effective strategy to prevent antibacterial resistance. Infection due to multi-drug resistance has become a burden worldwide, and patients treated with traditional antibiotics has become challenging and ineffective (Kadri et al. 2019). Traditional antibiotics are known for their molecular targets such as protein synthesis, cell wall synthesis, DNA replication, and various other biomolecular processes inside the bacterial cell (Sköld 2011; Walsh 2000). These molecular targets are modified by various modification processes such as gene transfer from resistive to non-resistive cells through plasma exchange, inactivating the antibiotics, or evacuate antibiotics out of the cell with the help of ABC transporter (Wink 2012). The advantage of the combination of antimicrobial drug over traditional antibiotics is that it affects molecular targets such as biomembrane, proteins, and DNA. This might help to conquer the antibiotic-resistance mechanisms, to expand the antibacterial spectrum, reduced toxicity, and reinstate the efficiency of antibiotics (Chan et al. 2011).

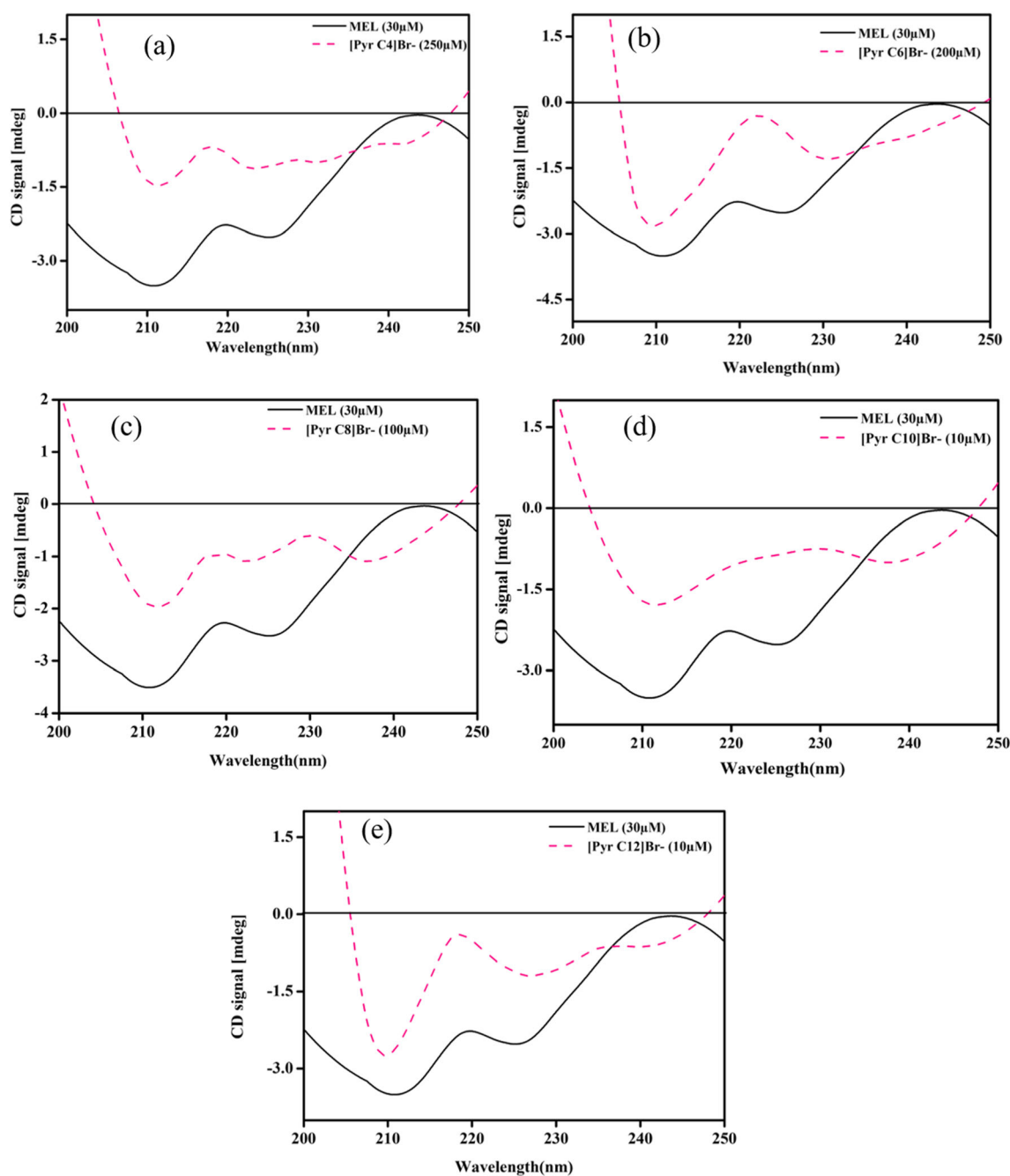


Fig. 7 Far-UV-CD spectra of MEL (30 μ M) in the presence and absence of different concentrations of (a) [Pyr C₄]Br⁻, (b) [Pyr C₆]Br⁻, (c) [Pyr C₈]Br⁻, (d) [Pyr C₁₀]Br⁻, and (e) [Pyr C₁₂]Br⁻ in 10 mM Tris buffer at 298 K and at pH 7.2

Earlier studies showed the synergistic effect of MEL with some antibiotics (Akbari et al. 2019). Recent studies related to synergism between MEL and doripenem the MIC value of MEL and doripenem decreased up to 61.6- and 51.3-fold, respectively, against *A. baumannii*, where they reported that the consumption of MEL has reduced to 61.6 folds (Issam et al. 2015). This subsequently causes a decrease in its cytotoxicity. Another study revealed the combination of MEL with colistin where it did not show any additive effect against bacterial burden (Akbari et al. 2019). This study showed the

application of MEL-doripenem as an antibacterial agent in the treatment of infections caused by *A. baumannii*. Therefore, there was an urgent need to develop the combination with MEL to achieve an agent that could work more than 61.6-fold against *Gram-negative* and *Gram-positive* bacteria.

Our previous study relates to developing a combination of two antibiotics, MEL and IL (best result was obtained with [PyrC₁₂NTf₃⁻]), where the reduction in bacterial burden was found to be up to 95%. This was the remarkable achievement in the study and reached to a combination which might reduce

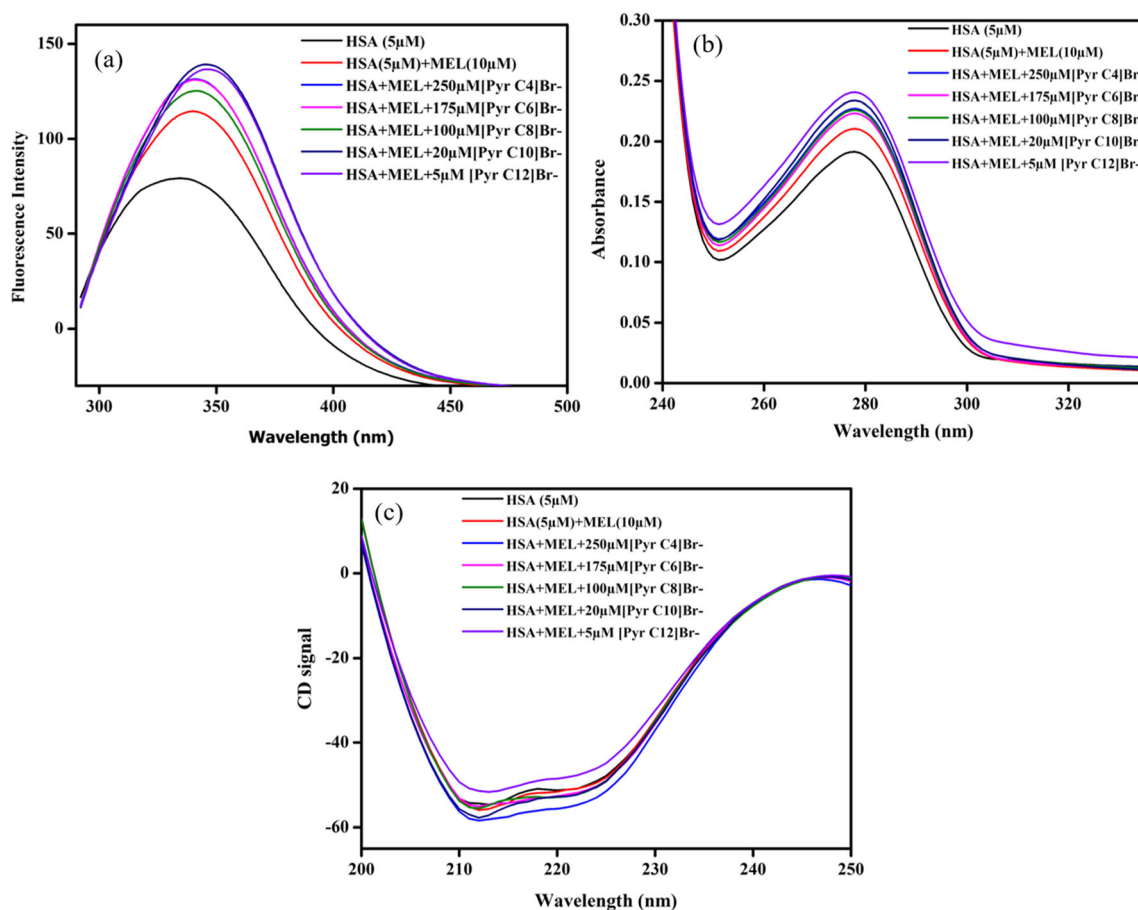


Fig. 8 (a) Absorption spectra, (b) fluorescence emission spectra, (c) far-UV-CD spectra of HSA (5 μM) and MEL (10 μM) in absence and presence of different concentrations of [Pyr C₁₂] Br⁻ at 298 K and at pH 7.2

the dose intake of MEL and will retrench the toxic effect. ILs are known for its adsorption characteristic whereas MEL for its pore formation mechanism. Our present study involved the synthesis of pyrrole-based ILs having Br⁻ as a counter ion. The best antibacterial combination was obtained when MEL was combined with IL having octyl, decyl, and dodecyl carbon chain. The reduction in bacterial burden was up to 90–92% which showed comparatively lesser efficiency to our previous results (Saraswat et al. 2020). The increased biological efficiency of the conjugate in the previous study may be due to the more hydrophobic counter (CF₃SO₂)₂N⁻ attached as compared with the Br⁻ with the cation moiety in the present study.

A previous study showed that the increased toxic effect of IL with (CF₃SO₂)₂N⁻ counterion is may be due to the increased hydrophobicity and fluorine atom present in the counter ion. In our study, we have used ILs contained Br⁻ as a counter ion and due to this, the cytotoxicity assay results showed less toxicity behavior of used ILs. Therefore, we tried the series of pyrrole-based ILs having Br⁻ as a counter ion as an effective antibacterial agent with MEL.

The inhibition of bacterial burden up to 90–92% was observed when treated with MEL in combination with [Pyr C₁₂]Br⁻. The presence of IL with MEL showed exceptional improvement in the MIC value of MEL. This will not only

Table 2 Stern-Volmer constant (K_{sv}), binding constant (K_b), number of binding sites n , and relative thermodynamic parameters for the [Pyr C₁₂]Br⁻ and MEL system at different temperatures and 7.2 pH

Temp (K)	K_{sv} ($L\text{mol}^{-1} s^{-1}$)	n	K_b ($L\text{mol}^{-1}$)	ΔS ($\text{kJK}^{-1} \text{mol}^{-1}$)	ΔH (kJmol^{-1})	ΔG (kJmol^{-1})	$K_a, UV\text{-Vis}$ ($L\text{mol}^{-1}$)
298	7.78×10^4	0.92	6.20×10^4	-795.68	-262.04	-24.93	30.46×10^4
303	4.03×10^4	0.76	0.25×10^4			-20.95	
308	3.45×10^4	0.66	0.09×10^4			-16.97	
313	2.57×10^4	0.57	0.01×10^4			-12.99	

decrease the dosage of either MEL or IL but will also exclude the chances of getting side effects. This will result in the formation of MEL-IL, as a potential therapeutic agent for the treatment of infections occurring due to *E. coli* and *S. aureus*. Improved antimicrobial efficiency of MEL-IL conjugate is more likely due to their target site on the cell wall. The action mechanism of IL is still unknown, but MEL is known for its pore-forming tendency on the cell wall. The improved efficacy of MEL-IL may be due to the reason that IL may be adding more absorption efficiency to MEL so that it may get more adsorbed on the cell membrane. The surface tension data and MIC data showed the dependence of MIC value on the surface activity of synthesized ILs. ILs with longer alkyl chain length has the highest tendency to get adsorbed on the cell membrane. Subsequently, MEL which is non-covalently attached to ILs could create a pore into the cell membrane and helps in entering of IL into the cell leading to leakage of cytoplasmic material and cell death. ILs with MEL showed a significant effect on the microbial activity of MEL. In the present study, all ILs with shorter chain length showed improved results in terms of MIC value of MEL but the best synergism was found when MEL and [Pyr C₁₂]Br⁻ within the tested range of concentrations. MEL-ILs conjugate adsorbs more on the cell wall, creating the pore inside the outer membrane of the bacterial cell due to increased absorption with increasing hydrophobicity, increased migration rate, and dispersed charge. The aforesaid mode of action is more like to administrate the penetration of MEL to reach the cell wall leading to disruption of the cell wall and cell death. The development of bacterial resistance is due to the genetic and climatic modifications. The gene exchange from resistive to non-resistive bacterial cells favours bacterial resistance (Munita and Arias 2016) which is more likely to stop the plasma exchange between the cells and might help in decreasing bacterial resistance.

The present study concludes with the successful synthesis of the pyrrolidinium-based ILs followed by the characterization. The cytotoxicity result revealed the lesser toxicity of synthesized ILs over imidazolium- and pyridinium-based ILs. The antimicrobial assay results showed the greater efficiency of ILs having longer chain length in comparison with the ILs having shorter chain length towards both the bacterial strains. Further, the microbial activity of MEL in the presence of ILs gave the unique composition of all synthesized ILs and MEL. In the present study, we have reported the best antibacterial combination as MEL and [Pyr C_x]Br⁻ comprising of a combination of 0.77 μM MEL+100 μM [Pyr C₈]Br⁻, 0.62 μM MEL+20 μM [Pyr C₁₀]Br⁻, 0.52 μM MEL+10 μM [Pyr C₁₂]Br⁻ against *E. coli* and 0.62 μM MEL+20 μM [Pyr C₁₀]Br⁻, 0.63 μM + 10 μM [Pyr C₁₂]Br⁻ against *S. aureus* which further did not showed any growth after 24 h. The improved MIC value of MEL with synthesized ILs will suppress the dose intake of MEL. Subsequently, lower the

toxicity, in turn, will decrease the chances of developing resistance towards bacterial strains. The combination of MEL and ILs display a possible cost-effective and eco-friendly antibacterial composition within the tested concentration range. Besides, the haemocompatibility assay suggested the compatibility of MEL-IL conjugate with human albumin. Also, the binding studies suggested the stability of the composition formed. Overall, their pharmacological and safety properties suggest that the conjugates of MEL with ILs will hopefully lead to the development of a therapeutic agent in the area of healthcare for the treatment of infections and will exclude the risk of bacterial resistance.

Acknowledgements This research was supported by the Researchers Supporting Project number (RSP-2020/35), King Saud University, Riyadh, Saudi Arabia. Dr. Rajan Patel greatly acknowledges the financial support from the Science and Engineering Research Board (EEQ/2016/000339) New Delhi, India. Juhi Saraswat is also thankful to the ICMR, New Delhi, India, for providing a research grant (F. No.45/19/2019-BIO/BMS).

Author contribution JS performed the whole experimental part and wrote the manuscript.

KI performed the cytotoxicity experiment in the study.

MA wrote the cytotoxicity part in the manuscript.

SYA and BA help to revise the manuscript.

RP is the corresponding author.

Compliance with ethical standards

Conflict of interest The authors declare that they have no conflict of interest.

Ethical statement This article does not contain any studies with human participants or animals performed by any of the authors.

References

- Akbari R, Hakemi-Vala M, Pashaie F, Bevalian P, Hashemi A, Pooshang Bagheri K (2019) Highly synergistic effects of melittin with conventional antibiotics against multidrug-resistant isolates of *acinetobacter baumannii* and *pseudomonas aeruginosa*. *Microb Drug Resist* 25(2):193–202
- Behera K, Pandey S (2007) Concentration-dependent dual behavior of hydrophilic ionic liquid in changing properties of aqueous sodium dodecyl sulfate. *J Phys Chem* 111(46):13307–13315
- Bhat AR, Wani FA, Alzahrani KA, Alshehri AA, Malik MA, Patel R (2019) Effect of rifampicin on the interfacial properties of imidazolium ionic liquids and its solubility therein. *J Mol Liq* 292: 111347
- Chan BC, Ip M, Lau CB, Lui S, Jolivald C, Ganem-Elbaz C, Litaudon M, Reiner NE, Gong H, See RH (2011) Synergistic effects of baicalein with ciprofloxacin against NorA over-expressed methicillin-resistant *Staphylococcus aureus* (MRSA) and inhibition of MRSA pyruvate kinase. *J Ethnopharmacol* 137(1):767–773
- Chemical SR (2014) Technological challenges in antibiotic discovery and development: a workshop summary. National Academies Press (US)

- Clinical, Institute LS (2012) Methods for dilution antimicrobial susceptibility tests for bacteria that grow aerobically; Approved Standard M7-A9, CLSI, Pennsylvania, USA
- Florio W, Becherini S, D'Andrea F, Lupetti A, Chiappe C, Guazzelli L (2019) Comparative evaluation of antimicrobial activity of different types of ionic liquids. *Mater Sci Eng C* 104:109907
- Garcia MT, Ribosa I, Perez L, Manresa A, Comelles F (2013) Aggregation behavior and antimicrobial activity of ester-functionalized imidazolium-and pyridinium-based ionic liquids in aqueous solution. *Langmuir* 29(8):2536–2545
- Garcia MT, Ribosa I, Perez L, Manresa A, Comelles F (2017) Micellization and antimicrobial properties of surface-active ionic liquids containing cleavable carbonate linkages. *Langmuir* 33(26):6511–6520
- Gbaj AM (2018) Differentiation between natural and commercial bee venoms using fluorescence spectroscopy
- Hughes D, Karlén A (2014) Discovery and preclinical development of new antibiotics. *Ups J Med Sci* 119(2):162–169
- Issam A-A, Zimmermann S, Reichling J, Wink M (2015) Pharmacological synergism of bee venom and melittin with antibiotics and plant secondary metabolites against multi-drug resistant microbial pathogens. *Phytomedicine* 22(2):245–255
- Kadri SS, Strich JR, Swihart BJ, Hohmann S, Dekker JP, Palmore T, Bonne S, Freeman B, Raybould J, Shah NG (2019) Attributable mortality from extensively drug-resistant *Gram-negative* infections using propensity-matched tracer antibiotic algorithms. *Am J Infect Control* 47(9):1040–1047
- Khameneh B, Diab R, Ghazvini K, Bazzaz BSF (2016) Breakthroughs in bacterial resistance mechanisms and the potential ways to combat them. *Microb Pathog* 95:32–42
- Khara JS, Wang Y, Ke X-Y, Liu S, Newton SM, Langford PR, Yang YY, Ee PLR (2014) Anti-mycobacterial activities of synthetic cationic α -helical peptides and their synergism with rifampicin. *Biomaterials* 35(6):2032–2038
- Khawam A, Flanagan DR (2006) Solid-state kinetic models: basics and mathematical fundamentals. *J Phys Chem* 110(35):17315–17328
- Kumari M, Maurya JK, Tasleem M, Singh P, Patel R (2014) Probing HSA-ionic liquid interactions by spectroscopic and molecular docking methods. *J Photochem Photobiol B* 138:27–35
- Maisetta G, Mangoni ML, Esin S, Pichierrì G, Capria AL, Brancatisano FL, Di Luca M, Barnini S, Barra D, Campa M (2009) In vitro bactericidal activity of the N-terminal fragment of the frog peptide esculentin-1b (Esc 1–18) in combination with conventional antibiotics against *Stenotrophomonas maltophilia*. *Peptides* 30(9):1622–1626
- Maurya JK, Mir MUH, Maurya N, Dohare N, Ali A, Patel R (2016) A spectroscopic and molecular dynamic approach on the interaction between ionic liquid type gemini surfactant and human serum albumin. *J Biomol Struct Dyn* 34(10):2130–2145
- Maurya N, Maurya JK, Singh UK, Dohare R, Zafaryab M, Moshahid Alam Rizvi M, Kumari M, Patel R (2019) In vitro cytotoxicity and interaction of noscapine with human serum albumin: effect on structure and esterase activity of HSA. *Mol Pharm* 16(3):952–966
- Morrisett JD, David JS, Pownall HJ, Gotto AM Jr (1973) Interaction of an apolipoprotein (apoLP-alanine) with phosphatidylcholine. *Biochemistry* 12(7):1290–1299
- Munita JM, Arias CA (2016) Mechanisms of antibiotic resistance. *Microbiol Spectr* 4(2):1–24
- Nascimento GG, Locatelli J, Freitas PC, Silva GL (2000) Antibacterial activity of plant extracts and phytochemicals on antibiotic-resistant bacteria. *Braz J Microbiol* 31(4):247–256
- Omoya FO, Ajayi KO (2016) Synergistic effect of combined antibiotics against some selected multidrug resistant human pathogenic bacteria isolated from poultry droppings in Akure, Nigeria. *Adv Appl Microbiol* 6(14):1075–1090
- Organization WH (2019) Environmental aspects of manufacturing for the prevention of antimicrobial resistance. *WHO Drug Inform* 33(4):709–712
- Patel R, Mir MUH, Maurya JK, Singh UK, Maurya N, Mud P, Khan AB, Ali A (2015) Spectroscopic and molecular modelling analysis of the interaction between ethane-1, 2-diyl bis (N, N-dimethyl-N-hexadecylammoniumacetoxo) dichloride and bovine serum albumin. *Luminescence* 30(8):1233–1241
- Patel R, Maurya N, Mud P, Farooq N, Siddique A, Verma KL, Dohare N (2018) Esterase activity and conformational changes of bovine serum albumin toward interaction with mephedrone: spectroscopic and computational studies. *J Mol Recognit* 31(11):e2734
- Payne DJ (2008) Desperately seeking new antibiotics. *Science* 321(5896):1644–1645
- Qin J, Guo J, Xu Q, Zheng Z, Mao H, Yan F (2017) Synthesis of pyrrolidinium-type poly (ionic liquid) membranes for antibacterial applications. *ACS Appl Mater Interfaces* 9(12):10504–10511
- Regmi S, Choi YH, Choi YS, Kim MR, Yoo JC (2017) Antimicrobial peptide isolated from *Bacillus amyloliquefaciens* K14 revitalizes its use in combinatorial drug therapy. *Folia Microbiol* 62(2):127–138
- Reinhardt A, Horn M, Schmauck JP, Brohl A, Giernoth R, Oelkrug C, Schubert A, Neundorff I (2014) Novel imidazolium salt–peptide conjugates and their antimicrobial activity. *Bioconjug Chem* 25(12):2166–2174
- Ross PD, Subramanian S (1981) Thermodynamics of protein association reactions: forces contributing to stability. *Biochemistry* 20(11):3096–3102
- Saraswat J, Wani FA, Dar KI, Rizvi MMA, Patel R (2020) Noncovalent conjugates of ionic liquid with antibacterial peptide melittin: an efficient combination against bacterial cells. *ACS Omega* 5(12):6376–6388
- Sharma T, Dohare N, Kumari M, Singh UK, Khan AB, Borse MS, Patel R (2017) Comparative effect of cationic gemini surfactant and its monomeric counterpart on the conformational stability and activity of lysozyme. *RSC Adv* 7(27):16763–16776
- Sköld O (2011) Antibiotics and antibiotic resistance. Wiley Online Library
- Spellberg B, Bartlett JG, Gilbert DN (2013) The future of antibiotics and resistance. *N Engl J Med* 368(4):299–302
- Walsh C (2000) Molecular mechanisms that confer antibacterial drug resistance. *Nature* 406(6797):775–781
- Wani FA, Khan AB, Alshehri AA, Malik MA, Ahmad R, Patel R (2019) Synthesis, characterization and mixed micellization study of benzene sulphonate based gemini surfactant with sodium dodecyl sulphate. *J Mol Liq* 285:270–278
- WHO AR (2014) Global Report on Surveillance. Antimicrobial resistance, Global Report on Surveillance
- Wink M (2012) Secondary metabolites from plants inhibiting ABC transporters and reversing resistance of cancer cells and microbes to cytotoxic and antimicrobial agents. *Front Microbiol* 3:130
- Zhang S-K, Ma Q, Li S-B, Gao H-W, Tan Y-X, Gong F, Ji S-P (2016a) RV-23, a Melittin-related peptide with cell-selective antibacterial activity and high hemocompatibility. *J Microbiol Biotechnol* 26(6):1046–1056
- Zhang S-K, J-w S, Gong F, Li S-B, Chang H-Y, Xie H-M, Gao H-W, Tan Y-X, Ji S-P (2016b) Design of an α -helical antimicrobial peptide with improved cell-selective and potent anti-biofilm activity. *Sci Rep* 6:27394